ELSEVIER

Earth and Planetary Science Letters 168 (1999) 255–270

EPSL

Tectonic segmentation of the North Andean margin: impact of the Carnegie Ridge collision

M.-A. Gutscher [a,*], J. Malavieille [a], S. Lallemand [a], J.-Y. Collot [b]

[a] *Laboratoire de Géophysique et Tectonique, UMR 5573, Université Montpellier II, Place E. Bataillon, F-34095 Montpellier, Cedex 5, France*

[b] *IRD, Geosciences Azur, Villefranche-sur-Mer, France*

Received 17 July 1998; accepted 2 March 1999

Abstract

The North Andean convergent margin is a region of intense crustal deformation, with six great subduction earthquakes $M_w \geq 7.8$ this century. The regional pattern of seismicity and volcanism shows a high degree of segmentation along strike of the Andes. Segments of steep slab subduction alternate with aseismic regions and segments of flat slab subduction. This segmentation is related to heterogeneity on the subducting Nazca Plate. In particular, the influence of the Carnegie Ridge collision is investigated. Four distinct seismotectonic regions can be distinguished: Region 1 – from 6ºN to 2.5ºN with steep ESE-dipping subduction and a narrow volcanic arc; Region 2 – from 2.5ºN to 1ºS showing an intermediate-depth seismic gap and a broad volcanic arc; Region 3 – from 1ºS to 2ºS with steep NE-dipping subduction, and a narrow volcanic arc; Region 4 – south of 2ºS with flat subduction and no modern volcanic arc. The Carnegie Ridge has been colliding with the margin since at least 2 Ma based on examination of the basement uplift signal along trench-parallel transects. The subducted prolongation of Carnegie Ridge may extend up to 500 km from the trench as suggested by the seismic gap and the perturbed, broad volcanic arc. These findings conflict with previous tectonic models suggesting that the Carnegie Ridge entered the trench at 1 Ma. Furthermore, the anomalous geochemical (adakitic) signature of the volcanoes in the broad Ecuador volcanic arc and the seismicity pattern are proposed to be caused by lithospheric tears separating the buoyant, shallowly subducting Carnegie Ridge from segments of steep subduction in Regions 1 and 3. It is further suggested that Carnegie Ridge supports a local 'flat slab' segment similar to that observed in Peru. The impact of the Carnegie Ridge collision on the upper plate causes transpressional deformation, extending inboard to beyond the volcanic arc with a modern level of seismicity comparable to the San Andreas fault system. The pattern of instrumental and historical seismicity indicates (1) great earthquakes on the northern and southern flanks of the colliding ridge, (2) a slight reduction in observed seismicity at the trench–ridge intersection, (3) increased stress far into the continent, and (4) a NNE displacement of the N. Andes block, to be further effects of the collision.

Keywords: Northern Andes; plate collision; tectonics; seismicity; segmentation; earthquakes

* Corresponding author. Fax: +33-467-523908; E-mail: malavie@dstu.univ-montp2.fr

0012-821X/99/$ – see front matter
PII: S0012-821X(99)00060-6

1. Introduction and tectonic setting

The North Andean margin is a region of intense crustal deformation, in particular where Carnegie Ridge is subducting beneath Ecuador (Fig. 1). This section of the subduction zone has produced six great (defined as $M_w > 7.75$) earthquakes this century. The largest in 1906 ($M_w = 8.8$) had an estimated rupture zone of ca. 500 km length, partially reactivated in three subsequent events from south to north, in 1942, 1958 and 1979 [1,2]. This region, frequently cited when discussing models of segment rupture, earthquake propagation and recurrence intervals [1–4], was also the site of the large $M_w = 7.1$ earthquake, August 4, 1998. The region of greatest seismicity coincides with the subducted northern flank of Carnegie Ridge. Unlike other subduction zones, in the North Andes instrumental and histori-

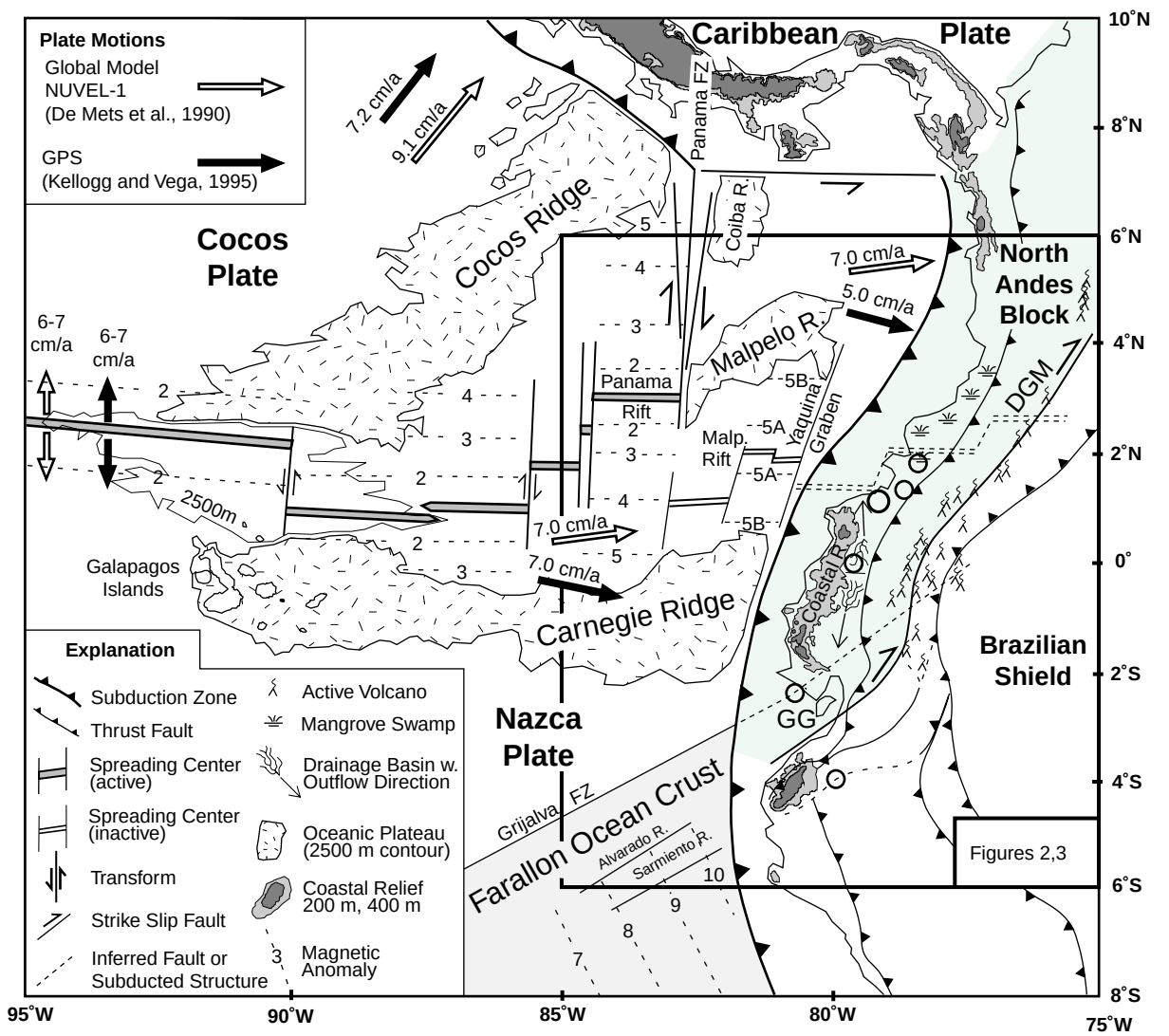

Fig. 1. Tectonic setting of the study area showing major faults, relative plate motions according to GPS data [7] and the NUVEL-1 global kinematic model [8], magnetic anomalies [13] and active volcanoes [50]. Here and in Fig. 4, the locations of the 1906 ($M_w = 8.8$, very large open circle) and from south to north, the 1953, 1901, 1942, 1958 and 1979 ($M \geq 7.8$, large open circles) earthquakes are shown. *GG* = Gulf of Guayaquil; *DGM* = Dolores–Guayaquil Megashear.

cal seismicity $M \geq 7$ extend hundreds of kilometers inland and beyond the volcanic arc. The current debate on seismic coupling in subduction zones [5,6] and its relation to subducting bathymetric highs (asperities) bears strongly on the entire area and on the assessment of its seismic risk.

Recent advances in instrumentation and computer technology and availability of satellite-derived data present a unique opportunity to combine independent, high resolution, digital data sets from a variety of fields (seismology, volcanology, morphology/topography, satellite altimetry, GPS–geodetic studies, structural geology) for application to geodynamic problems. The principal objective of this study is to re-examine the seismicity and tectonics in this region of intense crustal deformation in view of these newly available data. By studying the spatial distribution of hypocenters and examining focal mechanisms we aim to identify the principal fault planes, identify areas prone to large earthquakes and scrutinize apparent seismic gaps. Correlations between structural heterogeneity of the oceanic Nazca Plate and uplift, deformation and volcanism in the overriding South American Plate should improve our understanding of these processes and of the overall lithospheric structure of an oceanic plateau–subduction zone collision.

Along the North Andean margin, the Nazca Plate is subducting eastwards beneath South America at a rate of 5–7 cm/a [7,8] (Fig. 1). Simultaneously, the North Andean block is being displaced to the northeast at a rate of ca. 1 cm/a along the Dolores–Guayaquil Megashear accounting for the discrepancy between the global model (Nazca motion relative to stable South America) [2] and the GPS measurements (Nazca motion relative to the North Andes block [7,9] (Fig. 1). Thus, the ENE-oriented Carnegie Ridge is sweeping southwards along the Ecuador margin. Recent coastal uplift facing Carnegie Ridge is indicated by Pliocene marine terraces (Tablazos) exposed at 200–300 m elevations [10,11]. To the north, the morphology, widespread mangrove swamps and neotectonics of the South Colombian coastal block, suggest active subsidence [11].

The most widely accepted tectonic model for the formation of the oceanic crust of the E. Panama Basin suggests that a major plate reorganization took place ca. 25 Ma, breaking the Farallon Plate into the Cocos and Nazca plates to the south and the Juan de Fuca Plate farther to the north [12]. Due to differential stresses on the northeastward-subducting Cocos Plate and the eastward-subducting Nazca Plate, spreading was initiated around 23 Ma between the two plates in the vicinity of the Galapagos hotspot and later evolved into the current-day Galapagos Rift with N–S spreading [13,14]. The Grijalva scarp, an old N60°E fracture zone in the Farallon Plate, is interpreted to represent the southern half of the scar where the Nazca Plate tore off. Carnegie and Cocos ridges are mirror-image hotspot traces formed by the northeastward motion of the Cocos Plate and the eastward motion of the Nazca Plate over the Galapagos hotspot [13–16]. According to this model both Cocos and Carnegie ridges arrived at their respective trenches 1 Ma [13].

Most models suggest that Malpelo Ridge is a former continuation of Cocos Ridge separated by dextral motion along the N–S-trending Panama FZ [13,14]. Malpelo and Carnegie ridges separated from one another during a period of rifting and seafloor spreading from ca. 17 to 8 Ma [13,15,17]. The expressions of the extinct Malpelo Rift and adjacent rift segments as well as the transform faults separating them are clearly visible in the morphology of the seafloor (Fig. 2).

2. Seismicity database and observations

Earthquake data in the study area were obtained from Engdahl et al.'s recent global relocation effort [18], improving hypocenter locations from the International Seismological Centre (ISC) Catalog. Thus, for this study area 1230 events $M_b > 4.0$ from January 1964 to December 1995 were available. Catalogs of lesser quality but (1) covering a greater time span (the South American SISRA Catalog [19] ca. 800 events $M_b > 4.0$ from 1900 to 1972), or (2) comprising more events (the USGS PDE – Preliminary Determination of Earthquakes – Catalog; ca. 1800 events $M_b > 4.0$ from 1973 to 1997), were also examined and revealed the same overall distribution patterns, though with inferior spatial resolution and well known 'artifacts' such as large concentrations of events at depths of 33 km or 15 km.

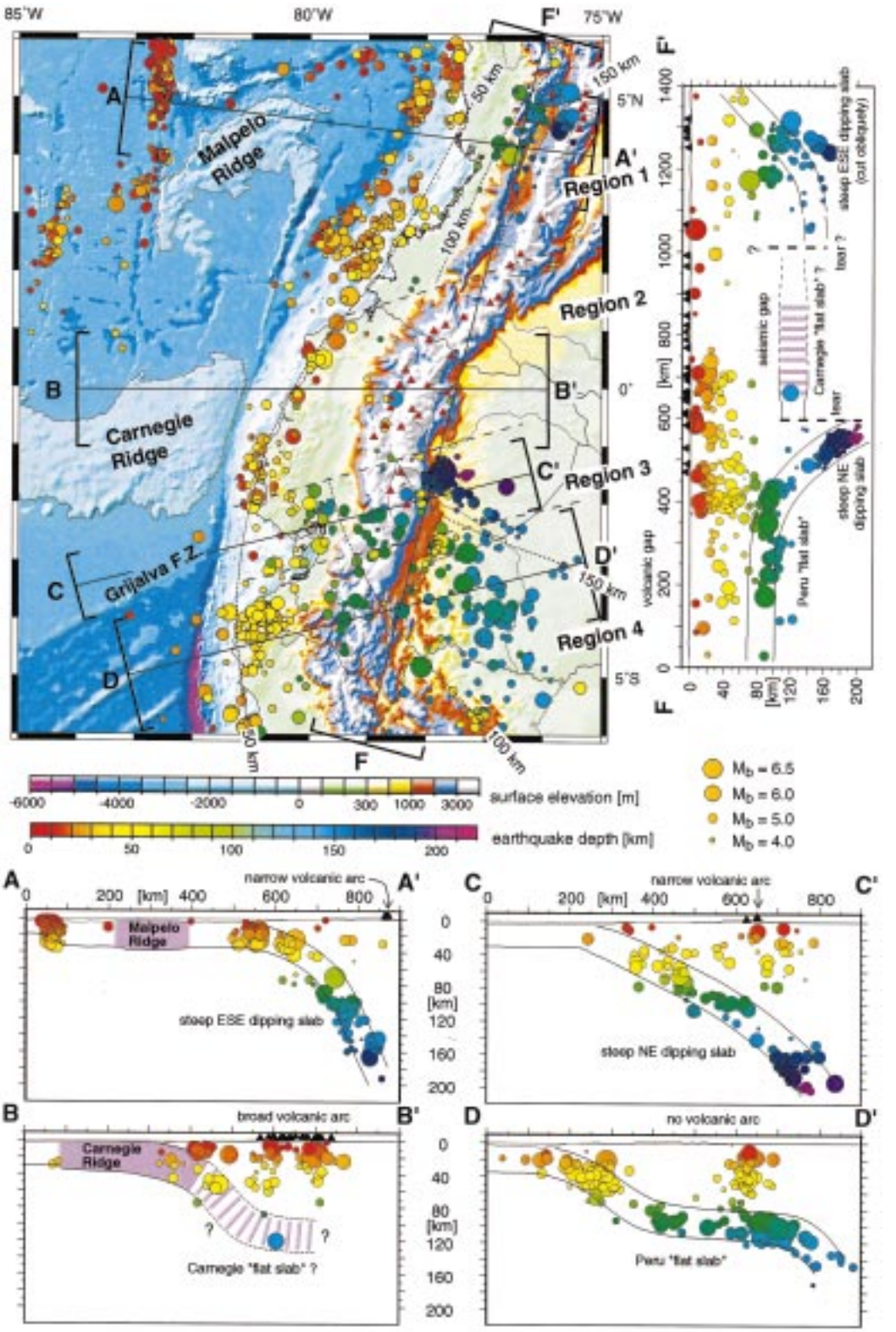
85°W
80°W
75°W
5°N
0°
5°S
A
A'
B
B'
C
C'
D
D'
F
F'
Malpelo Ridge
Carnegie Ridge
Grijalva F.Z.
Region 1
Region 2
Region 3
Region 4
50 km
100 km
150 km
seismic gap
Carnegie "flat slab" ?
tear ?
steep ESE dipping slab (cut obliquely)
steep NE dipping slab
Peru "flat slab"
volcanic gap
[km]
surface elevation [m]
earthquake depth [km]
M_b = 6.5
M_b = 6.0
M_b = 5.0
M_b = 4.0
narrow volcanic arc
broad volcanic arc
no volcanic arc
steep ESE dipping slab
steep NE dipping slab
Carnegie "flat slab" ?
Peru "flat slab"

The EHB database [18] is shown sorted by magnitude and hypocenter depth and was used to calculate depth contours to the Wadati–Benioff zone (Fig. 2). Four different regions, with distinct patterns of seismicity and volcanic activity [15,20] are observed from north to south. Representative lithospheric cross-sections based on the seismicity, volcanism and topography databases are presented to illustrate these main differences (Fig. 2).

Region 1, Section A–A′. The northernmost region (in west-central Colombia) shows a steep ESE-dipping Wadati–Benioff zone down to a depth of about 200 km in good agreement with earlier seismological [15] and recent tomographic results [21]. The volcanic arc is narrow and located above a slab at ca. 160 km depth. Malpelo Ridge and the active Panama FZ lie west. Lithospheric ages (<5 Ma) and thicknesses (<20 km) are least to the west since nearby at the Panama Rift, new oceanic lithosphere is currently forming (Fig. 1).

Region 2, Section B–B′. Between 2.5ºN and 1ºS there is a nearly complete absence of intermediate depth seismicity (only one event >90 km depth). The seismic gap is confirmed by the SISRA and PDE catalogs as well as by a local seismological network of 54 stations operated during the Lithoscope experiment [22]. Carnegie Ridge enters the trench across from the broad (160 km wide), adakitic volcanic arc. The inferred subducted continuation of Carnegie Ridge is interpreted to be a 'flat slab' configuration, but is constrained by only a single major event $M_b = 5.8$ at 120 km depth.

Region 3, *Section C–C′*. Between 1ºS and 2ºS there is cluster of intermediate-depth seismicity defining a steep NE-dipping slab. South of Carnegie Ridge the transition from young to older oceanic lithosphere (Grijalva FZ) is crossed. The narrower 1.2º sampling width and ENE alignment clearly image a steep-dipping slab segment with its narrow overlying arc.

Region 4, Section D–D′. South of 2ºS the Peru 'flat slab' segment begins, with a volcanic gap all the way to 15ºS in southern Peru [23–26]. Nearly horizontal subduction is observed, despite the greater age and presumably greater density and thickness of Farallon crust. Recent work suggests that this 1500 km long 'flat slab' is supported by two buoyant oceanic plateaus, the completely subducted Inca Plateau in N. Peru and the currently subducting Nazca Ridge in S. Peru [27]. Since no intervening wedge of asthenospheric material is present between the downgoing Nazca Plate and the overriding South American Plate, partial melting is inhibited and no arc develops. Shallow events (<40 km) in the E. Andes (between km 700 and 780) appear to represent intracontinental 'subduction' where the Brazilian shield underthrusts the Andes at a rate of ca. 1.5 mm/a, producing crustal-scale thrust slices [28].

While the northern two sections are oriented nearly parallel to the relative convergence direction between the North Andes block and the Nazca Plate [7,9], the southern sections are oriented ENE–WSW in order to better sample the particular region. Note that the 'seismological thickness' of the subducting oceanic lithosphere in all profiles is ca. 30 km, as pointed out by earlier investigators [23]. This corresponds roughly to the effective elastic thickness (T_e) of the lithosphere as related to its thermal age through well known cooling relationships. For a 40 Ma oceanic lithosphere an effective elastic thickness of ca. 25 km is predicted for a wet olivine mantle rheology, while a 100 Ma lithosphere is predicted to have $T_e = 35$ km [29].

Finally, the Andes parallel section F–F′ (Fig. 2) also clearly illustrates the principal differences between the four regions. Furthermore, it implies that

Fig. 2. Shaded hill relief and seismicity of the study area. Bathymetry and topography from Smith and Sandwell's TOPEX database [51] with active volcanoes (red triangles) [50]. Seismicity (1964–1995), 1230 events $M_b > 4.0$, from Engdahl et al.'s global hypocenter relocation [18] scaled by depth and magnitude, omitting upper plate seismicity (<70 km depth >200 km east of the trench) in map. Oceanic plateaus defined by 2500 m contour. Location and sampling boxes of seismological sections indicated. Depth contours to the Wadati–Benioff zone indicated as dotted lines. Seismotectonic Regions 1–4 (see text) also shown. Section *A–A′*, *Region 1*, steep ESE-dipping subduction, narrow volcanic arc. Section *B–B′*, *Region 2*, intermediate-depth seismic gap, subduction of Carnegie Ridge with inferred flat slab shown, broad volcanic arc is spread out over 150 km. Section *C–C′*, *Region 3*, narrow volcanic arc, steep NE-dipping slab. Section *D–D′*, *Region 4*, Peru flat slab segment, no volcanic arc. Section *F–F′*, Andes-parallel profile illustrating the intermediate depth seismic gap and inferred Carnegie 'flat slab' in Region 2. Note the tear north of the steep NE-dipping slab in Region 3.

Table 1
Listing of events and fault plane solutions obtained from the Harvard CMT catalog [30]

Event No.	Date (d/m/y)	Time GMT	Lat. (°)	Long. (°)	Depth (km)	M_b	M_w	Fault plane 1 strike/dip/slip (°)	Fault plane 2 strike/dip/slip (°)	Notes mech./loc.
1	30/07/80	06:56	5.18	−82.70	18.0	5.8	6.3	4/72/−171	272/81/−19	SS PanFZ
2	26/11/83	09:22	3.96	−82.52	32.7	5.4	5.6	174/83/173	265/83/8	SS PanFZ
3	12/12/88	13:32	5.31	−82.49	6.2	5.3	5.6	181/90/180	271/90/0	SS PanFZ
4	04/02/89	19:24	5.81	−82.63	10.9	5.8	6.3	93/76/10	0/80/166	SS PanFZ
5	20/07/90	04:05	4.70	−82.63	1.0	5.0	5.1	176/90/180	266/90/0	SS PanFZ
6	15/08/77	20:23	2.66	−84.51	17.7	5.2	5.0	251/45/−90	71/45/−90	N PanRift
7	18/09/92	10:50	3.39	−82.96	22.2	5.1	5.4	254/45/−90	74/45/−90	N PanRift
8	08/05/77	16:45	−1.25	−81.08	29.6	5.1	5.5	336/16/63	184/76/97	T subd
9	01/03/79	14:33	0.61	−80.06	9.6	5.6	5.7	23/24/116	175/69/79	T subd
10	12/12/79	08:00	1.57	−79.36	26.6	6.4	7.9	30/16/118	181/76/83	T subd
11	26/01/80	15:27	2.27	−79.57	26.1	5.0	5.6	12/22/76	207/69/95	T subd
12	06/05/81	21:36	−1.92	−80.94	15.1	6.0	6.4	339/17/81	168/73/93	T subd
13	10/06/85	03:23	3.00	−78.51	29.2	5.6	5.5	32/19/125	176/74/79	T subd
14	25/08/90	11:43	5.75	−77.53	28.4	5.1	5.3	350/36/79	183/54/98	T subd
15	02/09/90	04:27	−0.16	−80.25	14.6	5.8	6.2	22/27/115	174/65/78	T subd
16	19/11/91	22:29	4.53	−77.38	25.0	6.5	7.2	13/13/95	188/77/89	T subd
17	07/07/81	10:25	2.71	−79.82	17.8	5.1	5.3	16/43/−78	180/48/−101	N Yaq. B
18	12/02/89	20:03	2.77	−79.76	4.9	5.0	5.1	340/46/−116	195/50/−66	N Yaq. B
19	09/09/89	01:40	2.46	−79.73	14.8	6.0	5.7	1/29/−123	218/66/−73	N Yaq. B
20	26/11/94	04:48	2.87	−79.43	15.9	5.1	5.3	357/37/−114	206/57/−73	N Yaq. B
21	13/11/95	12:36	2.92	−79.39	17.6	5.3	5.3	208/45/−90	28/45/−90	N Yaq. B
22	02/01/81	07:37	2.12	−79.16	14.2	5.7	5.9	26/42/−128	252/58/−61	N tear?
23	07/01/81	07:01	1.98	−79.26	42.5	5.7	5.9	32/33/−114	240/60/−75	N tear?
24	18/08/80	15:08	−2.02	−80.04	55.5	5.5	5.9	19/27/36	256/75/−112	S tear?
25	27/06/81	21:54	−3.06	−80.28	53.1	5.1	5.3	298/30/−20	45/80/−119	S tear?
26	10/02/90	17:12	−3.20	−80.73	54.7	5.6	5.5	138/58/167	235/79/32	S tear?
27	19/05/83	19:07	0.14	−77.10	24.1	5.6	5.2	60/49/129	189/54/54	ST EAnd
28	06/03/87	01:54	−0.01	−77.66	12.2	6.1	6.4	198/20/118	348/73/81	T EAnd
29	06/03/87	04:10	0.04	−77.78	19.5	6.5	7.1	195/27/98	7/64/86	T EAnd
30	06/03/87	08:14	0.07	−77.85	8.6	5.4	6.0	226/40/−166	125/81/−51	SS EAnd
31	11/08/90	02:59	−0.18	−78.53	20.2	5.0	5.1	323/45/53	190/55/122	ST Quit
32	22/09/87	16:21	−1.06	−78.01	19	5.8	6.0	197/42/129	330/59/61	ST IAD
33	26/12/92	14:57	−1.01	−78.02	6.8	5.8	5.4	200/46/166	300/80/45	ST IAD
34	17/01/84	16:19	−3.93	−81.40	35.4	5.9	5.5	303/45/78	139/47/101	T Amot
35	29/07/90	15:29	−4.94	−81.00	41.5	5.4	5.2	10/17/58	223/76/99	T Amot
36	29/03/91	20:13	−3.98	−80.92	38.2	5.2	5.6	55/27/151	171/77/66	T Amot
37	11/04/82	12:21	−2.84	−78.63	15	5.4	5.1	39/26/56	256/68/106	T ASA
38	03/10/95	01:51	−2.83	−77.85	43.5	6.5	7.0	234/39/120	18/57/68	T SbAnd
39	03/10/95	12:45	−2.81	−77.82	15.2	6.0	6.4	243/45/157	349/74/47	ST SbAnd
40	08/10/95	10:27	−2.69	−77.89	33.6	5.3	5.4	240/80/−170	148/80/−10	SS SbAnd
41	31/03/83	13:13	2.41	−76.63	29.3	5.4	5.6	26/76/175	117/85/14	SS Col
42	06/06/94	20:47	2.79	−75.97	5.4	6.4	6.8	206/76/170	299/80/14	SS Col
43	20/04/80	11:26	−2.58	−78.52	101.1	5.1	5.2	151/35/−90	331/55/−93	dp.EcPer
44	08/10/80	22:01	−1.40	−77.63	199.5	5.5	6.0	115/16/−117	323/76/−82	dp.EcPer
45	03/11/81	07:02	−1.87	−78.36	141.8	5.5	5.9	133/28/−99	323/62/−85	dp.EcPer
46	18/11/82	14:57	−1.72	−76.65	193.2	6.0	6.5	163/29/−51	301/68/−109	dp.EcPer
47	12/04/83	12:07	−4.86	−78.10	90.3	6.5	7.0	339/35/−86	153/55/−93	dp.EcPer
48	11/09/93	06:14	−4.71	−76.27	120.2	5.6	5.7	154/44/−109	359/49/−73	dp.EcPer
49	29/05/79	12:59	5.24	−75.71	116.9	4.9	5.0	174/44/−100	8/47/−80	dp.Col
50	23/11/79	23:40	4.78	−76.17	107.8	6.4	7.2	137/41/−163	35/79/−51	dp.Col
51	25/06/80	12:05	4.48	−75.77	165.4	5.7	6.0	231/74/14	137/76/164	dp.Col
52	15/08/92	19:02	5.11	−75.60	116.8	5.7	5.9	228/22/−71	28/69/−97	dp.Col

Hypocenter locations from Engdahl et al. [18].

the continuation of Carnegie Ridge supports a local 'flat slab segment' at ca. 100–140 km depth, bounded to the south (and possibly to the north) by a lithospheric tear.

A total of 189 fault plane solutions for the study area were available from the Harvard centroid moment tensor (CMT) catalog [30] for the period January 1976–December 1997. A representative subset of 52 of these events is listed in Table 1 and shown in Fig. 3 using the more reliable EHB hypocenter locations [18] to highlight areas of particular interest and more complicated structure, not readily explained by current models.

In general, the mechanisms are consistent with the plate tectonic model of the study area. Several principal types can be distinguished: (1) shallow dextral strike-slip in the active Panama FZ (events 1–5); (2) shallow normal faulting in the active Panama Rift (events 6, 7); (3) shallow underthrusting in the subduction zone (events 8–16); (4) shallow normal faulting in the flexural bulge east of Yaquina Graben (events 17–21); (5) shallow thrusting and dextral strike-slip events in the upper plate (events 27–42); and (6) deeper, commonly normal faulting events in the downgoing slab (events 43–52).

3. Neotectonics and recent vertical motions

The 'basement uplift signal' of Carnegie Ridge was determined along a reference profile 100 km west of the trench and compared to profiles along a curved track parallel to the course of the Colombia Trench (Fig. 4). This was done to establish how far arc-ward the 'basement uplift signal' can be identified. Carnegie Ridge, together with the step from the Grijalva scarp, has a 400 km width and a height of ca. 2 km (Fig. 4a). The axial trench profile clearly shows the subducting ridge where the trench floor shallows by 1–1.5 km with respect to regions north and south (Fig. 4b). After adding the 1–1.5 km sedimentary fill at the trench north of the ridge, the full 2–2.5 km amplitude basement uplift signal is obtained. Beneath the Coastal Range 110 km from the trench, the regional bathymetric/topographic profile again shows a pronounced uplift in the continuation of the Carnegie Ridge (Fig. 4c). The elevations of the Coastal Range are ca. 1.5 km higher than the base level in the submarine regions at the northern end of the profile. If recent sedimentary fill is taken into account the difference is again 2–2.5 km. To the south the picture is obscured by the dramatic variations in basement level in and around the Gulf of Guayaquil. Here the 8 km deep Progreso Basin and the 10 km deep Jambeli and Esperanza basins in the Gulf of Guayaquil are believed to have formed as pull-apart basins within the strike-slip regime of the Dolores–Guayaquil Megashear (DGM) [31–33]. The signal of the Carnegie Ridge induced basement uplift is less clear in the Inland Valley profile 180 km east of the Colombia Trench (Fig. 4d). The basement is substantially higher in this region, but poorly constrained sediment thicknesses to the north, the 10 km deep Jambeli Basin to the south and the overlying Manabi Basin, render interpretation uncertain.

Pliocene marine terraces of the Tablazo Formation [10,11] exposed at 200–300 m elevation in the Coastal Range and the regional morphology are consistent with the southward migration of Carnegie Ridge according to the relative plate motions obtained by GPS measurements [7]. The young topography (in excess of 400 m) of the Coastal Range lies directly across the trench from Carnegie Ridge. To the north, in S. Colombia, the coastal block is currently subsiding as shown by vertical motions during the 1979 earthquake [34] and by the coastal mangrove swamps [13]. The margin here is also marked by large forearc basins [35,36] indicating subsidence of the former continental shelf. This pattern of recent uplift across from a subducting high and subsidence to the north indicates collision since at least 8 Ma.

4. Geodynamic model

Based on four principal pieces of evidence we propose that a prolongation of Carnegie Ridge has been subducting for at least 2 Ma and most likely 8 Ma to a position beneath the Andes, 400 km from the trench.

(1) The regional bathymetric/topographic profiles indicate a basement uplift signal comparable in size to Carnegie Ridge extending at least 110 km east from the trench. A N–S drainage divide 180 km east of the trench lies along the prolongation of the Carnegie Ridge crest.

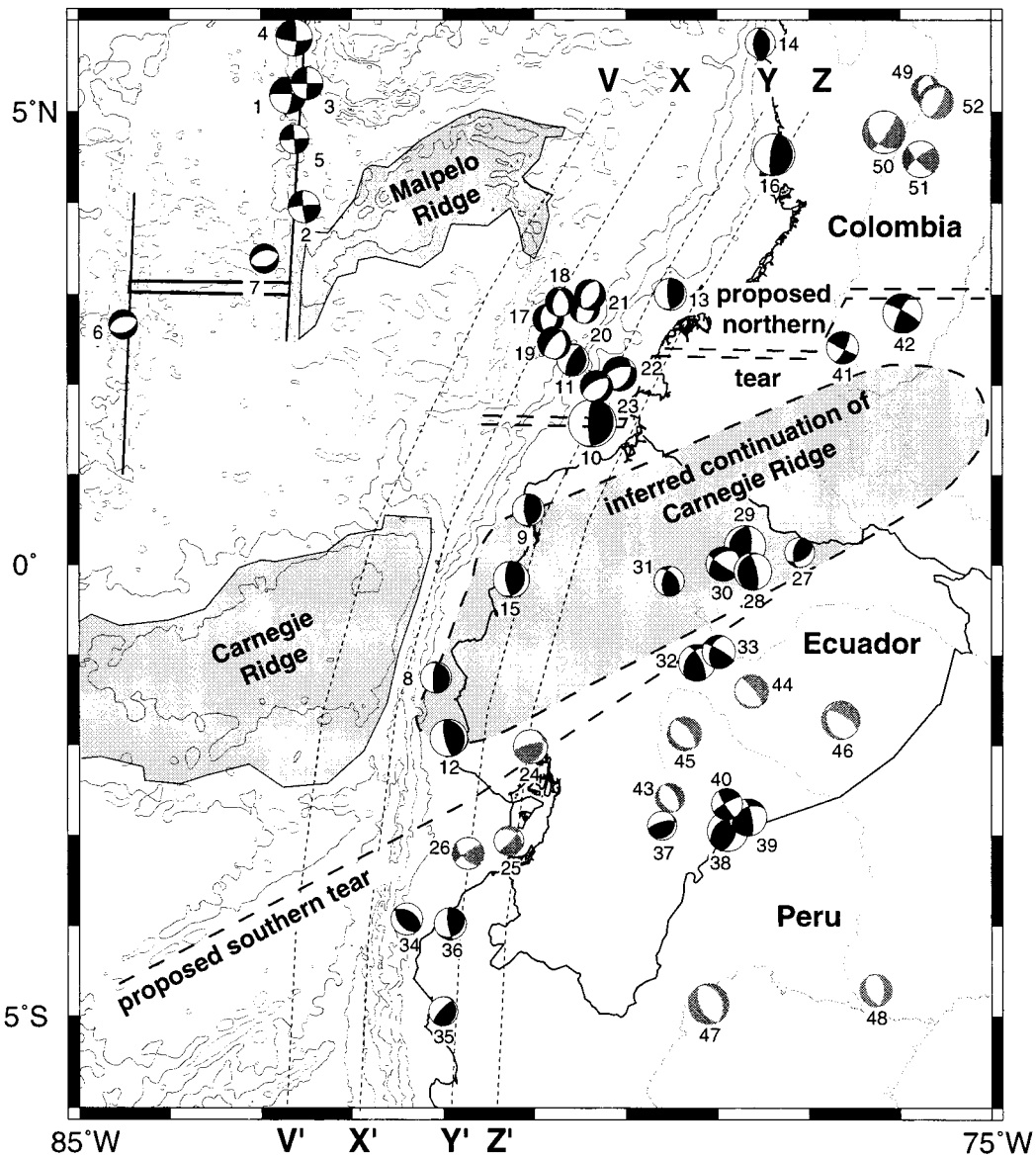

Fig. 3. Earthquake fault plane solutions from the Harvard CMT (centroid moment-tensor) [30] catalog. Solutions for shallow events (<50 km) are shaded black and deeper events (>50 km) gray, for 52 representative events listed in Table 1 using EHB [18] hypocenter locations. Several principal types can be distinguished: (1) shallow dextral strike-slip in the Panama FZ (events *1–5*); (2) shallow normal faulting in the Panama Rift (events *6*, *7*); (3) shallow underthrusting in the subduction zone (events *8–16*); (4) shallow normal faulting in the flexural bulge east of Yaquina Graben (events *17–21*); (5) shallow thrusting and dextral strike-slip in the upper plate (events *27–42*) and deeper, commonly normal faulting events in the downgoing slab (events *43–52*). Candidate tearing events in the north (events *22*, *23*) and south (events *24*, *25*) are indicated. Bathymetry (1000 m contours) [51] and location of regional topographic profiles (Fig. 4) also shown, with inferred positions of Carnegie Ridge prolongation and lithospheric tears dashed.

(2) The coastal morphology (Coastal Range uplift, subsidence to the north in the S. Colombian coastal block) are consistent with the southward migration of Carnegie Ridge according to relative plate motions and indicate collision since 8 Ma.

(3) A pronounced gap in intermediate depth (70–

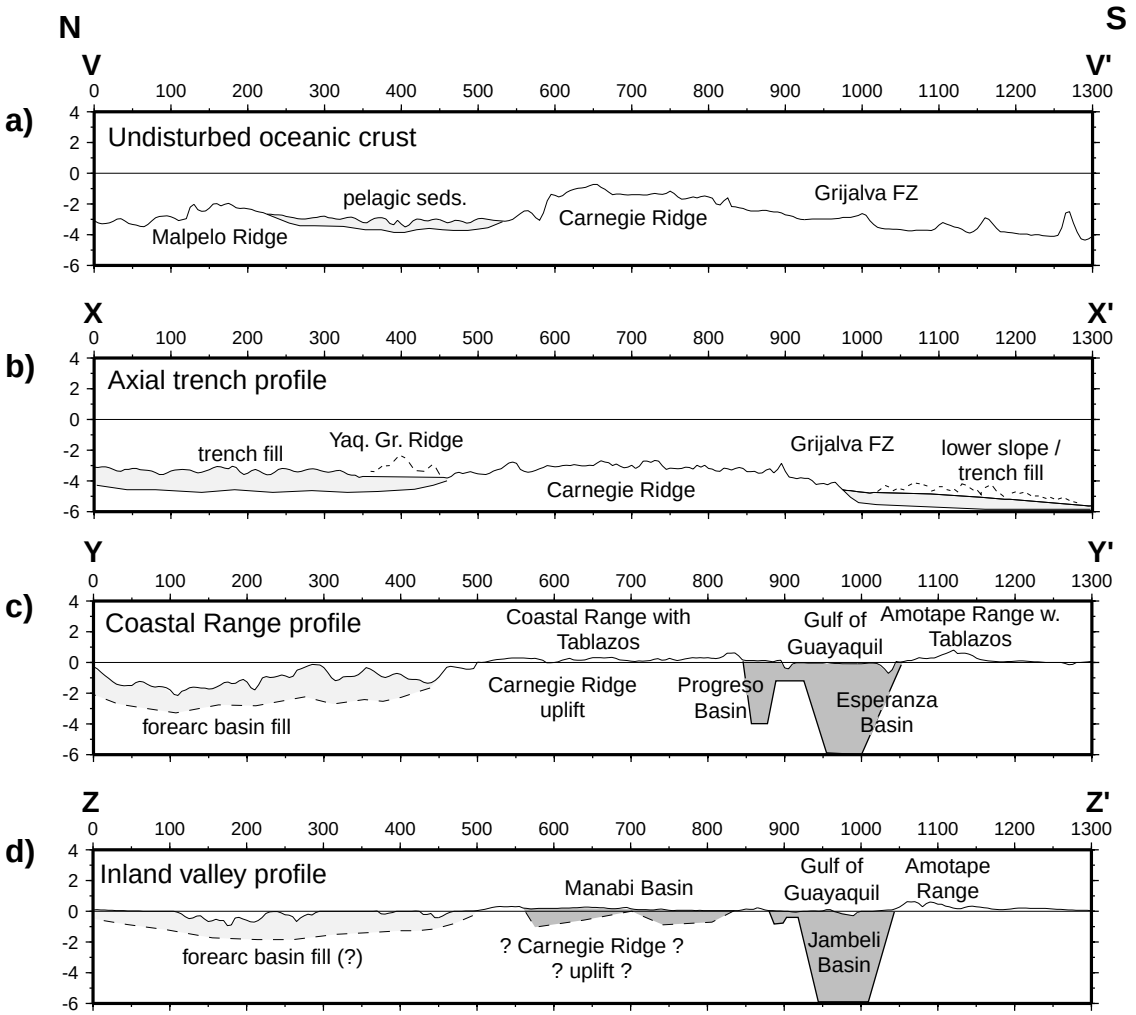

Fig. 4. Four regional topographic profiles parallel to the Colombia Trench axis (locations in Fig. 3). Basin and basement structure (for place names see Fig. 6) adopted from earlier studies [31–33]. (a) Section *V–V′*, undisturbed oceanic crust profile, 110 km west of the trench. Note Malpelo Ridge to the north and Grijalva FZ and two adjacent ridges in the Farallon Ocean Crust to the south. (b) Section *X–X′*, trench axial profile. Note ca. 1–1.5 km thick trench fill north of Carnegie Ridge [35,36] and south of Grijalva FZ [31]. The full 400 km × 2 km signal of the Carnegie Ridge is visible. (c) Section *Y–Y′*, Coastal Range profile, 110 km east of trench. Note the 1.5 km difference in the base level between the Coastal Range and the submerged coastal block in S. Colombia. (d) Section *Z–Z′*, Inland Valley profile, 180 km east of trench. Note the 8–10 km thick sediments in the Gulf of Guayaquil area at the southern end of the profile.

200 km) seismicity is observed in the prolongation of Carnegie Ridge, while normal seismicity continues in a steep (ca. 30º) Wadati–Benioff zone both north and south of this region. Seismic gaps are commonly observed where an oceanic plateau or other structural high (e.g. seamount chain, spreading center) collides with the trench [3,37].

(4) The active volcanic arc is broad (spread out over 150 km) and geochemically anomalous (see below). Therefore, some major geodynamic element is perturbing the system at depth.

The simple model of a continuation of Carnegie Ridge meets with two principal objections:

(1) It conflicts with the widely accepted view that the oceanic plateau terminates at the fossil Yaquina FZ and that collision with the trench began recently (1 Ma) [13,33].

(2) If Carnegie Ridge has been subducting for 8

Ma, why does arc volcanism continue in contradiction to the model of a ridge-induced volcanic gap [37]? And why is steep subduction [15,38] observed directly to the north and to the south?

The opinion that Carnegie Ridge does not continue east of the Yaquina Graben is based on geometric considerations, on poorly constrained magnetic anomaly data and on the presumption that the hotspot trace began at 25 Ma [13,17]. The 'termination model' further proposed that both Carnegie Ridge and Cocos Ridge (Costa Rica) entered their respective trenches at 1 Ma [13]. However, geological data on uplift rates in Costa Rica, indicating strong uplift as early as 3 Ma [16], contradict this interpretation for the Cocos Ridge collision and call into question its validity for the collision of its mirror image, Carnegie Ridge.

Recent studies suggest that the Caribbean Plateau is a large igneous province (LIP) formed as the plume head of the Galapagos hotspot rose to the surface, producing immense quantities of flood basalts in the Late Cretaceous ca. 90 Ma, [39,40]. Later Caribbean flood basalt-type magmatic events occurred from 76 Ma to 63 Ma [40]. Thus, if the hotspot was active in the Cretaceous and from late Tertiary to Quaternary times (25 Ma to present), it seems likely that the plume and associated hotspot trace existed between 60 Ma and 25 Ma. But if Carnegie Ridge has a subducted continuation as suggested by some workers [15,31,41], why does arc volcanism continue?

Ecuador arc magmas have an anomalous 'adakitic' geochemical signature requiring either unusually high temperatures allowing fusion of oceanic crust at shallow depths (<120 km) or a severe contamination by underplated basaltic crustal melts containing anomalously low concentrations of heavy rare earth elements [42]. However, a recent study on the geochemistry of Ecuador volcanoes virtually eliminates the possibility of crustal contamination and concludes that depth of melting is the predominant cause of geochemical variation [43]. It has been suggested in similar arcs showing adakitic signatures that a lithospheric tear or slab window is present allowing melting of the edges of the oceanic crust in contact with the hot asthenosphere below [44]. The geochemically anomalous melts originate at shallower depths and produce a broader volcanic arc than a typical subduction-related arc.

We propose a new model that combines the two ideas of a lithospheric tear and a continuation of Carnegie Ridge (Fig. 5). We suggest that two lithospheric tears bound the Carnegie Ridge collision zone. Melting of the oceanic lithosphere at the edges of the tears can thus explain the adakitic magmas observed within the broad volcanic arc of Ecuador. The southern tear, imaged in Fig. 2, occurs along the Grijalva FZ separating the Oligocene age Farallon crust to the southeast from the Cocos–Nazca crust (<25 Ma) to the northwest as has been suggested by previous workers [15,20]. The older, denser Farallon crust between 2ºS and 0.5ºS plunges steeply to the northeast. The northern tear in the lithosphere is tentatively located just north of the Carnegie Ridge along the extension of the Malpelo Rift fossil spreading center. To the north of this region the Cocos–Nazca crust (possibly attached to older Farallon crust at depth) subducts steeply to the east-southeast. Between these two tears we propose a flat slab segment with a configuration similar to that observed in Peru and central Chile. The buoyant prolongation of the Carnegie Ridge is interpreted to continue at least 110 km and probably up to 500 km from the trench (Figs. 3 and 5). An analysis of density and buoyancy in subduction zones suggests that oceanic plateaus must have a basaltic crustal thickness in excess of 17 km in order to resist subduction [45]. The western portion of Carnegie Ridge beneath the Galapagos Islands reaches a maximum crustal thickness of 18 km [46] and, though no geophysical data are available on the crustal structure at the eastern end of the ridge, it is presumably similar.

An alternative hypothesis of 'slab detachment' also succeeds in explaining many of the seismological and volcanological observations. This hypothesis is based in part on the ridge termination model [13] and presumes that at a short distance from the trench (ca. 100 km) Carnegie Ridge ends abruptly and that further to the east there is a section of denser, Eocene age Farallon crust. The older, denser lithosphere may have broken off and be sinking into the mantle creating a slab window above. This slab window would be responsible for the intermediate-depth seismic gap and would allow fusion of the edges of the oceanic crust producing the adakitic signature in the volcanic arc at the surface. However, we favor the two-tear model, because it implies a continuity of Carnegie

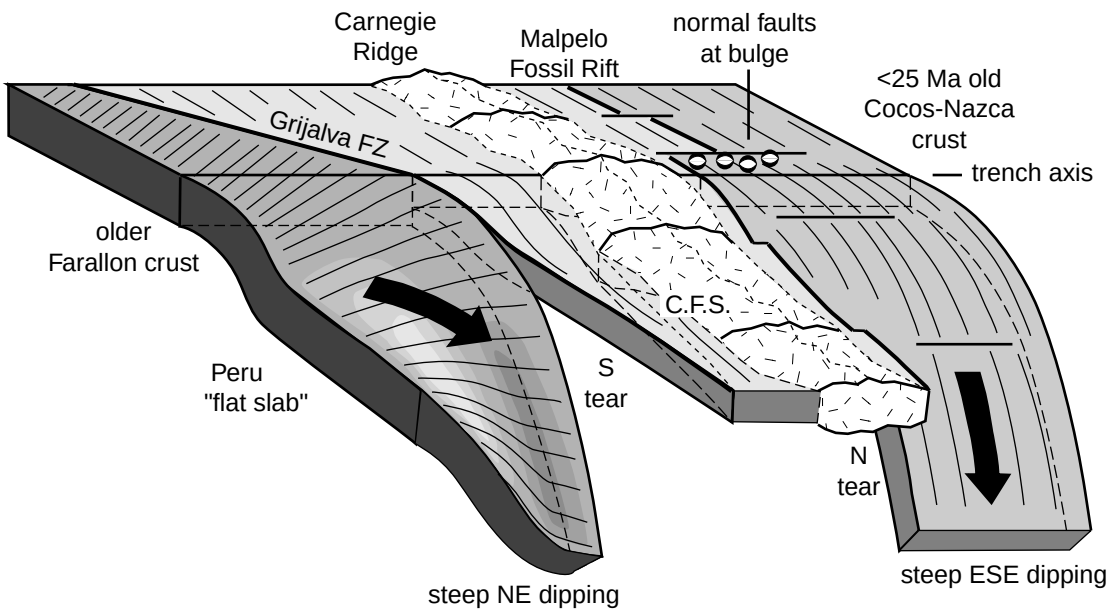

Fig. 5. 3-D view of the two-tear model for the Carnegie Ridge collision featuring: a steep ESE-dipping slab beneath central Colombia; a steep NE-dipping slab from 1ºS to 2ºS; the Peru flat slab segment south of 2ºS; a northern tear along the prolongation of the Malpelo fossil spreading center; a southern tear along the Grijalva FZ; a proposed Carnegie flat slab segment (*C.F.S.*) supported by the prolongation of Carnegie Ridge.

Ridge with the Caribbean–Galapagos Plume trace and thus succeeds in explaining the coastal pattern of subsidence to the north and uplift in the coastal range in accordance with a southward-sweeping of Carnegie Ridge.

The proposed lithospheric tears can be expected to produce earthquakes with a steep E–W-striking focal plane and a steep slip vector. Such 'tearing events' would be the only definitive validation of the model. While no such events have been reported in earlier studies, two candidate events occurred in N. Ecuador in January 1981, ($M_b = 5.6$–5.7) with a focal plane striking N70ºE and steep 60º dip (events 22, 23 in Table 1 and Fig. 3). They occurred in the S. Colombian forearc at depths of 14 and 43 km in the vicinity of subduction zone thrust earthquakes (Fig. 3). They cannot be extensional events due to flexure of the oceanic lithosphere because (a) the flexural bulge is located 100 km further west (see events 17–21 in Fig. 3), and (b) the fault plane solutions are distinctly different (Fig. 3). Since extension along the conjugate N30ºE focal plane seems unlikely given the WNW–ESE compressional stress field, down to the north motion along the N70ºE-striking fault is more plausible.

Another supporting observation is the substantial seismicity in the flexural bulge (five normal events $M_b = 5.1$–6.0 between 1981 and 1995), limited to a ca. 100 km long segment of Nazca Plate east of the Yaquina Graben (Fig. 3). This area corresponds to Region 1 where the oceanic lithosphere subducts most steeply and thus flexure is the greatest. Yet seismic activity appears to terminate southwards near the proposed lithospheric tear. We interpret this pattern and the normal mechanisms as indications that the lithosphere just north of the tear is subject to the greatest flexural stresses causing surficial extension in the bulge. Further south the buoyant Carnegie Ridge causes the subducting slab to bend at a reduced angle of curvature, thus lowering the flexural stress in the bulge (Fig. 5).

There are candidate 'tearing events' to the south (events 24–26 in Table 1 and Fig. 3) with a NE–SW-striking focal plane (parallel to the Grijalva FZ trend) and down to the south sense of motion. They are located at 53–56 km depth and have sub-vertical fault planes dipping 75–80º. The substantial depth, and their position well west of the Andes indicate that they are within the downgoing oceanic litho-

sphere. Additionally, there is a band of seismicity paralleling the Grijalva FZ and extending from the Gulf of Guayaquil down to the 200 km deep cluster seismicity (from event 26 to 44 in Fig. 3). This suggests that the opening of the Gulf of Guayaquil and its 10–12 km deep basins may be a surface expression of the lithospheric tear at depth.

5. Interplate coupling and impact on the upper plate

The Carnegie Ridge collision appears to have affected the coupling between the Nazca and South American plates. Four great earthquakes have occurred on the northern flank of the collision (1906, 1942, 1958 and 1979), and one has occurred along the southern flank (1901) (though the magnitude and location for the latter are uncertain). None of these events appears to have ruptured across the ridge itself. This pattern is similar to the Nazca Ridge collision in S. Peru. During the last 60 years four great earthquakes $M_w \geq 7.8$ occurred north of Nazca Ridge and two to the south, but again no shock appears to have ruptured across the ridge–trench intersection [1,4].

The recent shallow (<70 km) seismicity in Ecuador suggests a gap between 1ºN and 0.8ºS (Fig. 2). This appears to confirm the model that the subduction/collision of bathymetric highs locally increases coupling [6] and causes short-term seismic gaps. Recurrence intervals in such zones of increased coupling may be as much as twice as long and thus exceed 100 years, leading to gaps in recent seismicity maps. Greater stress accumulation during an aseismic period implies accordingly greater stress release during rupture [6]. Indeed the August 4, 1998 ($M_w = 7.1$) event at 0.5ºS occurred in an apparently quiet region, but which had been correctly identified by Nishenko in 1991 [47] as a region with a 66% probability of a large or great earthquake before 1999.

On the other hand, the regions between 1º and 2ºS and between 4º and 6ºS appear to be failing frequently by moderate earthquakes (10 events and 23 events, respectively, $M_b > 5.0$ within 100 km from the trench from 1964 to 1995) and do not appear to present a major seismic risk. However, the Gulf of Guayaquil segment of the subduction zone (from 2.2ºS to 3.8ºS) has seen no earthquakes $M_b > 5.0$ in the past 30 years. Either this region is largely aseismic, due perhaps to the propagating lithospheric tear here or, here too, seismic coupling may be quite high and possibly building up to a magnitude 7 or greater event. The SISRA catalog [19] indicates that two very large, shallow earthquakes, $M \geq 7.4$ occurred near 3.5ºS in 1953 (Fig. 1) and 1959 and thus tends to support the latter interpretation.

Interplate coupling at a much deeper and larger scale may also be affected by the Carnegie Ridge collision. In the region facing Carnegie Ridge, increased upper plate seismicity and deformation extending 500–600 km inland to beyond the volcanic arc suggest the collision to be the driving mechanism behind the NE movement of the North Andean block. This movement is distributed along a network of transpressional faults at the southern edge of the N. Andes block [32,48,49] (Fig. 6). Individual fault splays visible in the morphology commonly correlate with bands of seismicity. Yet, some faults include segments of ca. 100 km length without recent activity (Fig. 6). These segments can also be considered potentially high risk areas.

Overall, the level of seismicity is comparable to that of the San Andreas fault. For a 500 km long segment of the DGM, 41 $M_b \geq 5.0$ and 5 $M_b \geq 6.0$ non-subduction related, shallow events (<70 km depth) occurred during the period January 1964–December 1995. Along the 800 km long segment of the San Andreas fault system from San Francisco to the Mexican border 80 $M_b \geq 5.0$ and 9 $M_b \geq 6.0$ events were recorded during the same 32 year period [18]. Historical intraplate seismicity in the Ecuadorian Andes is very high as well. Four earthquakes of intensity 7–8, five of intensity 9, three events of intensity 10 and one of intensity 11 struck the Andean region between 0º and 4ºS from 1541 to 1906 [1,19] (Fig. 6).

Unfortunately, little is known about the slip rates along individual faults and even less about the system as a whole. Two studies have attempted to constrain slip rates along these faults. The first one, along a splay of the Pallatanga fault in the central Ecuador Andes, is based on displacement of morphological features and arrived at a slip rate of 3–4.5 mm/a [49]. The second study was performed along

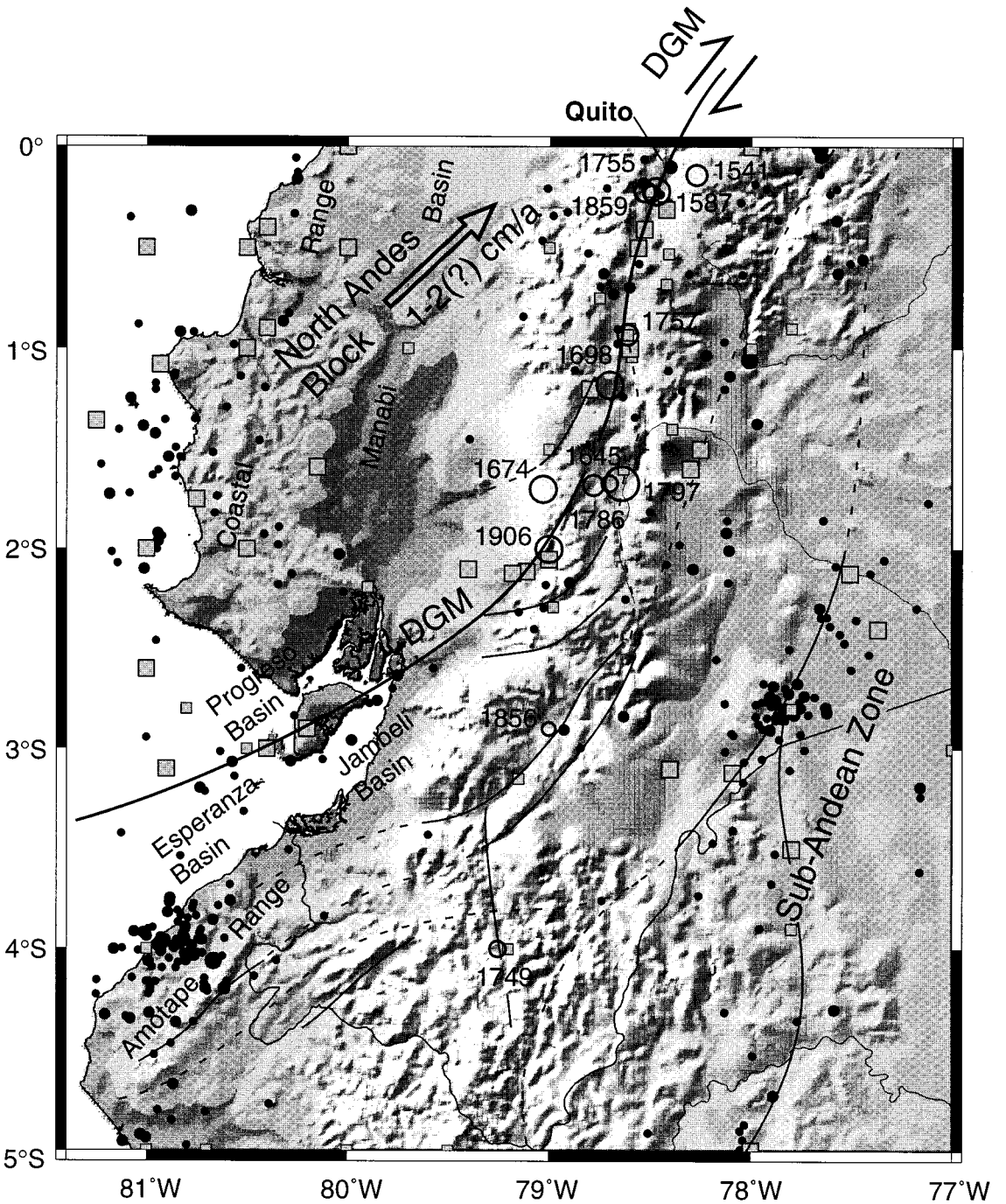

Fig. 6. Detailed topography and shallow (<70 km depth) seismicity of the Ecuadorian Andes showing known (solid) and inferred (dashed) faults. Dolores–Guayaquil Megashear (*DGM*) shown bold. *Pall.* F = Pallatanga Fault. Topography from GTOPO-30 digital database. Filled circles from the EHB data set (1964–1995) [18], $M_b \geq 4.0$ scaled by magnitude. Filled squares (1900–1963), $M_b \geq 5.0$ from the SISRA Catalog [19] scaled similarly. Unfilled black circles are epicenters of 13 large historical earthquakes from 1541 to 1906 from the SISRA Catalog [19] scaled according to magnitude and intensity from $M_I = 5.7$, $I = 7$ small circles to $M_I = 8.3$, $I = 11$ (largest circle – 1797).

the Rio Chingual–La Sofia fault at the Ecuador–Colombia border based on displacement of dated pyroclastic flows and arrived at a slip rate of 7 ± 3 mm/a [48]. However, in each case these are individual fault traces within a network of several faults and if all are active to a comparable degree then total displacement could approach 2 cm/a. The most reliable method to ascertain total strain rates would be a geodetic (GPS) study from the Brazilian craton across all the DGM fault splays. Given the high level of modern and historical intraplate seismicity in the Ecuadorian Andes such a study is warranted and necessary.

6. Conclusions

(1) The seismicity and active volcanism along the North Andean margin between 6ºN and 6ºS define four distinct regions.

- Region 1: from 6ºN to 2.5ºN, steep ESE-dipping subduction, narrow volcanic arc.
- Region 2: from 2.5ºN to 1ºS, intermediate depth seismic gap, broad volcanic arc.
- Region 3: from 1ºS to 2ºS, steep NE-dipping subduction, narrow volcanic arc.
- Region 4: south of 2ºS, Peru flat slab segment, no volcanic arc.

(2) A prolongation of Carnegie Ridge is proposed to continue >110 km beyond the trench. Four pieces of evidence support this conclusion.

(a) Coastal morphology: uplift in Coastal Range, subsidence in S. Colombian coastal block, consistent with southward migration of Carnegie Ridge according to GPS motions.

(b) Regional topography: a 400 km × 2 km basement uplift signal at least 110 km east of the trench.

(c) Seismicity pattern: intermediate depth seismic gap.

(d) Volcanic arc: a broad arc spread out over 150 km, the anomalous geochemistry of the arc magmas.

(3) The geodynamic segmentation and anomalous geochemistry (adakitic signature) of the arc magmas implies one or more lithospheric tears. The favored model involves two tears, at the boundaries between regions 1–2 and regions 2–3. The bowknot continuation of Carnegie Ridge is interpreted to support a local flat slab segment with melting of the oceanic plate at the edges of the tears producing adakitic magmas.

(4) Modern and historical intraplate seismicity is very high in the Ecuadorian Andes and in the network of NE-striking transpressive faults at the southern edge of North Andes block (five earthquakes $M_b > 6.0$ from 1964 to 1995). The transfer of deformation inland and the NE movement of the N. Andean block appear to be consequences of increased coupling from the Carnegie Ridge collision. In view of this significant activity, the deformation at the southern limit of the North Andes block should be quantified and the seismic risk along these faults reassessed.

Acknowledgements

M.-A. Gutscher's post-doctoral research was funded by a European Union TMR (Training and Mobility of Researchers) Stipend. Many thanks to J.-P. Eissen and E. Bourdon for stimulating discussions. Figures 2, 3, 4, 6 were produced using Wessel and Smith's GMT software. ***[AC]***

References

[1] J.L. Swenson, S.L. Beck, Historical 1942 Ecuador and 1942 Peru subduction earthquakes, and earthquake cycles along Colombia–Ecuador and Peru subduction segments, Pure Appl. Geophys. 146 (1996) 67–101.

[2] S.L. Beck, L.J. Ruff, The rupture process of the great 1979 Colombia earthquake: evidence for the asperity model, J. Geophys. Res. 89 (1984) 9281–9291.

[3] W.R. McCann, S.P. Nishenko, L.R. Sykes, J. Krause, Seismic gaps and plate tectonics: seismic potential for major boundaries, Pure Appl. Geophys. 117 (1979) 1083–1147.

[4] L.J. Ruff, Large earthquakes in subduction zones; segment interaction and recurrence times, in: G.E. Bebout, D.W. Scholl, S.H. Kirby, J.P. Platt (Eds.), Subduction: Top to Bottom, American Geophysical Union, Washington, DC, 1996, pp. 91–104.

[5] M. Cloos, R.L. Shreve, Shear-zone thickness and the seismicity of Chilean and Marianas-type subduction zones, Geology 24 (1996) 107–110.

[6] C.H. Scholz, C. Small, The effect of seamount subduction on seismic coupling, Geology 25 (1997) 487–490.

[7] J.N. Kellogg, V. Vega, Tectonic development of Panama, Costa Rica, and the Colombian Andes: constraints from Global Positioning System geodetic studies and gravity, in:

P. Mann (Ed.), Geologic and Tectonic Development of the Caribbean Plate Boundary in Southern Central America, Geol. Soc. Am. Spec. Pap. 295 (1995) 75–90.
[8] C. DeMets, R.G. Gordon, D.F. Angus, C. Stein, Current plate motions , Geophys. J. Int. 101 (1990) 425–478.
[9] J.T. Freymueller, J.N. Kellogg, V. Vega, Plate motions in the North Andean region, J. Geophys. Res. 98 (1993) 21853–21863.
[10] T. De Vries, The geology of late Cenozoic marine terraces (tablazos) in northwestern Peru, J. S. Am. Earth Sci. 1 (1988) 121–136.
[11] J.-F. Dumont, S. Benitez, et al., Neotectonics of the coastal region of Ecuador: a new pluridisciplinary research project, in: P.R. Cobbold et al. (Eds.), Third International Symposium on Andean Geodynamics (ISAG), St. Malo, Sept. 96, ORSTOM, France, 1996, pp. 175–178.
[12] R.N. Hey, Tectonic evolution of the Cocos–Nazca spreading center, Geol. Soc. Am. Bull. 88 (1977) 1414–1420.
[13] P. Lonsdale, K.D. Klitgord, Structure and tectonic history of the eastern Panama Basin, Geol. Soc. Am. Bull. 89 (1978) 981–999.
[14] T.W. Gardner, D. Verdonck, N.M. Pinter, R. Slingerland, K.P. Furlong, T.F. Bullard, S.G. Wells, Quaternary uplift astride the aseismic Cocos Ridge, Pacific coast, Costa Rica, Geol. Soc. Am. Bull. 104 (1992) 219–232.
[15] W.D. Pennington, Subduction of the eastern Panama Basin and seismotectonics of northwestern South America, J. Geophys. Res. 86 (1981) 10753–10770.
[16] R.A. Kolarsky, P. Mann, W. Montero, Island arc response to shallow subduction of the Cocos Ridge, Costa Rica, in: P. Mann (Ed.), Geologic and Tectonic Development of the Caribbean Plate Boundary in Southern Central America, Geol. Soc. Am. Spec. Pap. 295 (1995) 235–262.
[17] N.C. Hardy, Tectonic evolution of the easternmost Panama Basin: some new data and inferences, J. S. Am. Earth Sci. 4 (1991) 261–269.
[18] E.R. Engdahl, R.D. van der Hilst, R. Buland, Global teleseismic earthquake relocation with improved travel times and procedures for depth relocation, Bull. Seismol. Soc. Am. 88 (1998) 722–743. Online Data Set (available from E. Robert Engdahl, USGS) via anonymous ftp: ftp 136.177.20.1 cd misc/engdahl/EHB compressed hypocenter data file 1964–1995 (EHB.HDF) and format description (FORMAT.HDF)
[19] B.L. Askew, S.T. Algermissen (Eds.), Catalog of Earthquakes for South America: Hypocenter and Intensity Data. Ceresis Publication Volumes 4, 6 and 7a, b and c (1985). Online Data Set (Both SISRA and PDE Catalogs available from USGS National Earthquake Information Center): http://wwwneic.cr.usgs.gov/neis/epic/epic.html
[20] M.L. Hall, C.A. Wood, Volcano-tectonic segmentation of the N. Andes, Geology 13 (1985) 203–207.
[21] R. van der Hilst, P. Mann, Tectonic implications of tomographic images of subducted lithosphere beneath northwestern South America, Geology 22 (1994) 451–454.
[22] R. Prevot, J.-L. Chatelain, B. Guillier, H. Yepes, Tomographie des Andes équatoriennes: évidence d'une continuité des Andes Centrales, C.R. Acad. Sci. Paris 323 (1996) 833–840.
[23] M. Barazangi, B. Isacks, Spatial distribution of earthquakes and subduction of the Nazca plate beneath South America, Geology 4 (1976) 686–692.
[24] T. Cahill, B.L. Isacks, Seismicity and shape of the subducted Nazca Plate, J. Geophys. Res. 97 (1992) 17503–17529.
[25] E.R. Engdahl, R.D. van der Hilst, J. Berrocal, Imaging of subducted lithosphere beneath South America, Geophys. Res. Lett. 22 (1995) 2317–2320.
[26] R.H. Pilger, Plate reconstructions, aseismic ridges, and low-angle subduction beneath the Andes, Geol. Soc. Am. Bull. 92 (1981) 448–456.
[27] M.-A. Gutscher, J.-L. Olivet, D. Aslanian, J.-P. Eissen, R. Maury, Flat subduction beneath Peru caused by lost oceanic plateau, Nature (1999) in press.
[28] G. Suarez, P. Molnar, B.C. Burchfiel, Seismicity, fault plane solutions, depth of faulting, and active tectonics of the Andes of Peru, Ecuador and S. Colombia, J. Geophys. Res. 88 (1983) 10403–10428.
[29] B. Parsons, J.G. Sclater, An analysis of the variation of the ocean floor bathymetry and heat flow with age, J. Geophys. Res. 82 (1977) 803–827.
[30] A.M. Dziewonski, T.-A. Chou, J.H. Woodhouse, Determination of earthquake source parameters from waveform data for studies of global and regional seismicity, J. Geophys. Res. 86 (1981) 2825–2852. Online Data Set (available from Harvard University Centroid Moment Tensor – CMT Project): http://www.seismology.harvard.edu/projects/CMT/CMTsearch.html
[31] G.L. Shepherd, R. Moberly, Coastal structure of the continental margin, northwest Peru and southwest Ecuador, in: L. Kulm, J. Dymond, E.J. Dasch, D.M. Hussong (Eds.), Nazca Plate: Crustal Formation and Andean Convergence, Geol. Soc. Am. Mem. 154 (1981) 351–391.
[32] M. Daly, Correlations between Nazca/Farallon plate kinematics and forearc basin evolution in Ecuador, Tectonics 8 (1989) 769–790.
[33] A. Lavenu, T. Winter, F. Davilla, A Pliocene–Quaternary compressional basin in the Interandean Depression, Central Ecuador, Geophys. J. Int. 121 (1995) 279–300.
[34] D.G. Herd, T.L. Youd, H. Meyer, C.J.L. Arango, W.J. Person, C. Mendoza, The Great Tumaco, Colombia Earthquake of 12 December 1979, Science 211 (1981) 441–445.
[35] T.A. Minshull, S.C. Singh, G.K. Westbrook, Seismic velocity structure at a gas hydrate reflector, offshore western Colombia, from waveform inversion, J. Geophys. Res. 99 (1994) 4715–4734.
[36] N.P. Mountney, G.K. Westbrook, Quantitative analysis of Miocene to Recent forearc basin evolution along the Colombian convergent margin, Basin Res. 9 (1997) 177–196.
[37] S. McGeary, A. Nur, Z. Ben-Avraham, Spatial gaps in arc volcanism: the effect of collision or subduction of oceanic plateaus, Tectonophysics 119 (1985) 195–221.
[38] J. Vanek, V. Vankova, V. Hanus, Geochemical zonation of

volcanic rocks and deep structure of Ecuador and southern Colombia, J. S. Am. Earth Sci. 7 (1994) 57–67.
[39] N.T. Arndt, A.C. Kerr, J. Tarney, Dynamic melting in plume heads; the formation of Gorgona komatiites and basalts, Earth Planet. Sci. Lett. 146 (1997) 289–301.
[40] C.W. Sinton, R.A. Duncan, M. Storey, J. Lewis, J.J. Estrada, An oceanic flood basalt province within the Caribbean plate, Earth Planet. Sci. Lett. 155 (1998) 221–235.
[41] R.H. Pilger, Cenozoic plate kinematics, subduction and magmatism: South American Andes, J. Geol. Soc. London 141 (1984) 793–802.
[42] M. Monzier, C. Robin, M.L. Hall, J. Cotten, P. Mothes, J.-P. Eissen, P. Samaniego, Les adakites d'Equateur: modèle préliminaire, C.R. Acad. Sci. Paris 324 (1997) 545–552.
[43] R. Barragan, D. Geist, M. Hall, P. Larson, M. Kurz, Subduction controls on the composition of lavas from the Ecuadorian Andes, Earth Planet. Sci. Lett. 154 (1998) 153–166.
[44] S.T. Johnston, D.J. Thorkelson, Cocos–Nazca slab window beneath Central America, Earth Planet. Sci. Lett. 146 (1997) 465–474.
[45] M. Cloos, Lithospheric buoyancy and collisional orogenesis: subduction of oceanic plateaus, continental margins, island arcs, spreading ridges, and seamounts, Geol. Soc. Am. Bull. 105 (1993) 715–737.
[46] M.A. Feighner, M.A. Richards, Lithospheric structure and compensation mechanisms of the Galapagos Archipelago, J. Geophys. Res. 99 (1994) 6711–6729.
[47] S. Nishenko, Circum-Pacific seismic potential: 1989–1999, Pure Appl. Geophys. 135 (1991) 169–259.
[48] F. Ego, M. Sébrier, A. Lavenu, H. Yepes, A. Eques, Quaternary state of stress in the northern Andes and the restraining bend model for the Ecuadorian Andes, Tectonophysics 259 (1996) 101–116.
[49] T. Winter, J.-P. Avouac, A. Lavenu, Late Quaternary kinematics of the Pallatanga strike-slip fault (Central Ecuador) from topographic measurements of displaced morphological features, Geophys. J. Int. 115 (1993) 905–920.
[50] Smithsonian Global Volcanism Program, Online Data Set (available from Smithsonian Institution): http://www.volcano.si.edu/gvp/volcdata/index.htm
[51] W.H.F. Smith, D.T. Sandwell, Global seafloor topography from satellite altimetry and ship depth soundings, Science 277 (1997) 1956–1962.